Journal of Hydroscience and Hydraulic Engineering
Vol. 27, No.1 May, 2009, 1-10

DYNAMIC EFFECTS OF SUSPENDED SEDIMENTS ON TURBULENT FLOWS OVER DUNES

By

Kohtaro Chichibu

Ministry of Land, Infrastructure, Transport and Tourism
Hokkaido Bureau, Sapporo, Japan

Yasunori Watanabe

Associate Professor, Graduate School of Engineering
Hokkaido University, Sapporo, Japan

Yasuyuki Shimizu

Professor, Graduate School of Engineering,
Hokkaido University, Sapporo, Japan

SYNOPSIS

Quantitative momentum exchanges between water flow and suspended sand particles via dynamic interactions in open channel flows over sand dunes are discussed in this paper through comparisons of the velocities for water and sand phases over rigid and mobile dune beds. Velocities for both water and sand phases at the same locations were simultaneously measured in double camera PIV experiments using an optical resolution technique. The dynamic contributions of the suspended sediments to the carrier turbulent flows are discussed on the basis of the mean flow, turbulence statistics and relative velocity of the two phases. The local momentum exchanges between the sand and water flows via suspension, diffusion, settling and resuspension processes have important roles in determination of sand-laden turbulent flows over mobile sand dunes.

INTRODUCTION

Turbulence that has developed in the vicinity of a river sand-bed disturbs the bottom surface, which results in sand particles being carried downstream. The presence of suspended sand particles produces additional turbulence, resulting in modification of the carrier flow. Gore and Crow (1) showed that flow modification through particle-fluid interactions depends on the relative length of the turbulence scale and the particle size via kinetic energy exchange between the two phases.

On the other hand, the evolution of the turbulent boundary layer causes the formation of large-scale coherent structures involving turbulent bulges intermittently ejected via a bursting process, resulting in

excessive turbulent shear varying within the structure. On the mobile bed, the sediments are disturbed and eroded by the strong shear of the burst-forming vortices, resulting in the formation of periodic ramp-shaped bed geometry known as dunes.

In an open channel flow over a dune bed, the sediments suspended by energetic vortices separated behind the dune crest also locally modify carrier turbulent flow due to the drag acting on the sediments. Therefore, the fluid-solid interactions in turbulent flows involving separated vortices are responsible for determining local transport of the suspended sediments over an array of dunes.

There have been many attempts to experimentally determine fundamental features of the turbulence statistics of a single phase of water flows (without sediments) over a rigid model dune bed that was artificially formed (e.g., Schmeeckle 2). However, in order to elucidate the dynamic interaction and the resulting flow modifications over the dune bed, local motions of both suspended sand particles and water particles need to be simultaneously measured to estimate the velocity correlation between the two phases in the same flow and topographic conditions.

Particle imaging velocimetry (PIV) has been commonly used for measuring spatial distributions of particle velocities, and there have been many applications of PIV to open channel flows (e.g., Singh et al. 3, Nezu et al. 4). In this study, PIV was used for measuring simultaneous velocity distributions for both water and sand phases over a mobile dune bed on the basis of an optical resolution technique. The dynamic effects of the presence of suspended sand particles on carrier turbulent flows over the mobile dunes were quantitatively examined by making comparisons with flows for a single water phase over rigid impermeable dunes.

This paper is organized as follows. In section 2, the experimental setup and PIV technique are explained. The measurement results are discussed in section 3, and conclusions are presented in section 4.

EXPERIMENTS

We performed two experiments on open channel flows over artificial rigid and mobile sand dunes whose shapes are identical, with the aim of determining the effects of the suspended sand particles, permeability and roughness of the bed on turbulence statistics. The details of these experiments are described below.

Experimental setup

Experiments were conducted in a recirculating open channel of 10 m in length, 0.15 m in width and 0.3m in height with a uniform channel slope of 1/500 (see Figure 1). A sand layer of 5 cm in thickness was laid in a sand pit located in the middle section of the channel. The diameter and specific gravity of the sand particles used in the experiments were 0.34 mm and 2.61, respectively. Fluorescent neutral buoyant particles (mean diameter d=0.45 mm) were used as tracer particles of the water flow. The response of carrier flow to a particle is generally characterized by the Stokes number, which is the ratio of particle response time to a time characteristic of the fluid motion. The Stokes number (S_t), defined by $S_t = \frac{\rho_p d^2 U}{18\mu L}$ (ρ_p: the density of a particle, U: representative velocity and L: representative length scales of the carrier flow), for our neutral buoyant particles transported at mean streamwise velocity U=50cm/s with fluctuations at the length scale of mean wavelength of dunes L=24cm was estimated to be about 0.02, which is much smaller than unity. Therefore, the particle can maintains near velocity equilibrium with the carrier fluid.

The movements of the tracers and suspended sand particles, illuminated by a light sheet of a CW YAG laser, were recorded by two synchronized high-speed digital video cameras (250fps, resolution of 1K × 1K pixels). The cameras were adjacently mounted to record the same field of view (FOV) in the middle of the sand pit section. The FOV of a 10 cm square covered the region between the dune crest and trough under the light sheet (see Figure 1). The recorded images were sent to a PC via an image grabber connected to the cameras, which were converted into 8-bit gray-scale bitmap image.

An optical resolution technique was used to separately record each of the neutral buoyant tracer particles and suspended sand particles by two different cameras. Since the laser light, the wavelength of which is 532 nm, was directly reflected at the suspended sand particles, only the reflected light can be recorded by one camera equipped with an optical bandpass filter (bandpass range: 527–537 nm). The fluorescent tracer excited by the laser emits fluorescent light with the peak wavelength of about 570 nm. Therefore, by installing an optical high-pass filter (passing light at a wavelength 550 nm or longer) in another camera, only the fluorescent light emitted from the tracers can be captured and thus the reflected light from the sand particles is prevented from being recorded (see Figure 2).

Although a steady flow was discharged in the channel, the free surface was slightly disturbed owing to turbulence released from the bottom, causing a significant sway of the light sheet refracted at the disturbed surface, which increased out-of-plane error in the PIV procedure. An acrylic transparent board was installed at the level of the free surface to cover the surface under the laser illumination for stabilizing the surface and the position of the light sheet. It should be noted that although a laser illumination is possibly blocked by suspended sediments located near side of FOV in case of high sediment concentration, it never occurred in the present case.

Two experiments were performed by adopting the following procedures. (1) The motions of the fluorescent neutral tracer particles and sand particles over the mobile dune bed (MDB) were recorded by the two cameras when the flow and bed shape had achieved a quasi-steady state. (2) Water in the channel was drained immediately after the MDB experiment, and the sand surface was covered with cement powder to create a rigid impermeable thin layer over the dunes. (3) The single phase experiment to measure the motion of only the neutral tracers over the rigid dune bed (RDB) was performed at the same measurement location and the same discharge of 6.84 l/s as those used in the MDB experiment.

The water depths for the RDB and MDB were 104 mm and 112 mm, respectively. Typical two-dimensional shaped dunes with about 17 mm of wave height and 240 mm of wavelength have been formed in the channel. In the MDB, the sand particles were consecutively supplied at the upstream end of the channel to maintain a constant sand discharge. In this experiment, suspended-loads dominated the sediment transport process while bed-load was also observed on a rear surface of dunes (at a upstream side of the crest).

There could be a direct interaction between the tracer and suspended sand particles in dense particle flows. In this study, turbulence without the possible effect of the interaction in relatively dilute flows which is away from the mobile bed was discussed.

Image preprocessing

In the calibration procedure, a calibration board of 15 cm by 15 cm with square grids was installed on the measurement plane along the light sheet and was recorded by cameras to determine the calibration coefficients between the camera and real coordinates. The images which were captured were transformed on the basis of the perspective image projection with the calibration coefficients (see Figure 3). Image

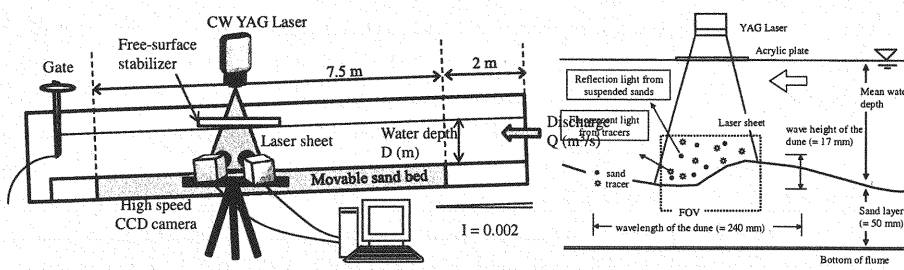

Figure 1: Experimental setup (left) and measurement region (right).

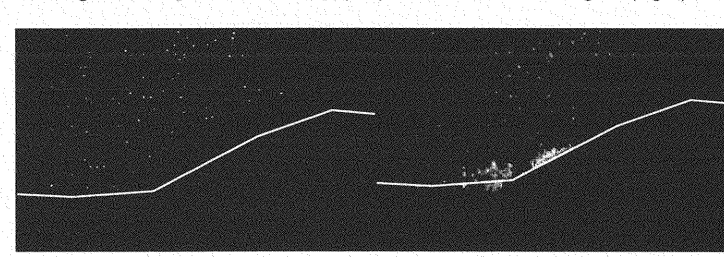

Figure 2: Example images of neutral buoyant tracers (left) and suspended sand particles (right) captured by two different cameras equipped with optical filters on the basis of the optical resolution technique.

noise was reduced by using a Gaussian digital filter.

In the measurement for the sand phase, the laser light reflected at the bottom continuously illuminated a fluid region near the bed during the measurement period (see Figure 2), which may reduce the cross-correlation of image patterns in the PIV procedure to increase the measurement error. The steady component of the reflected light was subtracted from the original images to eliminate the reflection effect.

Particle Imaging Velocimetry (PIV)

There have been many applications of PIV (particle image velocimetry) to engineering fields for measuring a plane distribution of a local flow. In this study, the standard PIV algorithm (cross-correlation method,

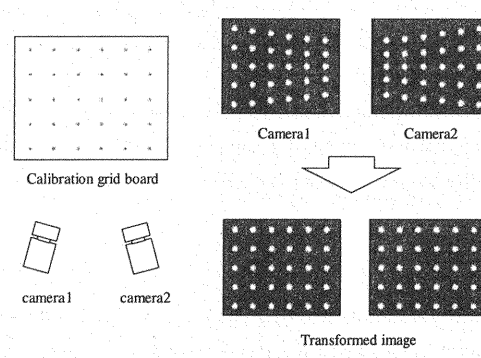

Figure 3: Schematic illustration of the image transformation from camera to real coordinates.

see Adrian 5) was used to estimate the velocities of both water particles and suspended sand particles. The normalized cross-correlation of image intensities between the interrogation area and search area for two consecutive frames is

$$C(\Delta x, \Delta y) = \frac{\sum_{i=1}^{N}\sum_{j=1}^{N}[f(x_i, y_j) - f_m][g(x_i + \Delta x, y_j + \Delta y) - g_m]}{\left(\sum_{i=1}^{N}\sum_{j=1}^{N}[f(x_i, y_j) - f_m]^2 \sum_{i=1}^{N}\sum_{j=1}^{N}[g(x_i + \Delta x, y_j + \Delta y) - g_m]^2\right)^{1/2}}, \quad (1)$$

where f and g denote the image intensities in the interrogation and search areas, and f_m and g_m represent the mean image intensities over the two areas, respectively. The sizes of the interrogation and search windows were 110 × 110 pixels (corresponding to a physical window of 10 × 10 mm) and 260 × 260 pixels, respectively. The overlapping rate of the interrogation window was 75%; the velocity was estimated at 2.5-mm spacing. The maximum correlation C_{max} was estimated at sub-pixel accuracy via a second-order interpolation. For the window location where C_{max} is greater than the threshold 0.7, the velocity is determined by

$$\boldsymbol{u} = \Delta \boldsymbol{x}_{max}/\Delta t, \quad (2)$$

where $\Delta \boldsymbol{x}_{max}$ is the interpolated displacement to give C_{max}. It was confirmed that the velocity estimated by (2) is unreliable if $C_{max} < 0.7$ or the total number of particles within the window was very small (less than 5). Therefore, rather than estimating the unreliable velocity, the new velocity is interpolated from the adjacent velocity by using the so-called square inverse distance method:

$$\boldsymbol{u}^*(x, y) = \frac{\sum_{ij} \boldsymbol{u}(x_i, y_j)/l^2}{\sum_{ij} 1/l^2}, \quad (3)$$

where $\boldsymbol{u}^*$ denotes the interpolated velocity, and $\boldsymbol{u}(x_i, y_j)$ is the reliable velocity with $C_{max} > 0.7$ around the location (x, y) at distance $l = \sqrt{(x - x_i)^2 + (y - y_j)^2}$.

A PIV standardization and popularization project (Visualization Society of Japan) has provided standard images of synchronized particle motion in given flows. Our PIV for the standard images was found to be capable of estimating the appropriate velocity; the correlation between the estimated and given velocities was 0.97 and the relative standard deviation of the velocities was 4.97%.

Turbulence statistics

Time-averaged turbulence properties over the measurement period of 10 s (2500 video frames) were statistically estimated for both water and sand phase velocities. It should be noted that the period is much longer than the time-scale of the turbulence involved in the separated vortices (less than 10 ms) and much shorter than the wave period of propagating dunes (about 20 min), which is an appropriate reference time-scale to define the quasi-steady flow over the dunes. The instantaneous velocities of water and sand can be written as

$$\boldsymbol{u}_f = \overline{\boldsymbol{u}}_f + \boldsymbol{u}'_f \quad (4)$$

$$\boldsymbol{u}_s = \overline{\boldsymbol{u}}_s + \boldsymbol{u}'_s, \quad (5)$$

where $\overline{u}$ is the time-averaged velocity and u' is the fluctuation component. The subscripts "f" and "s" denote the phases of fluid and sand, respectively. The turbulence energy (k) and Reynolds stress (R) for

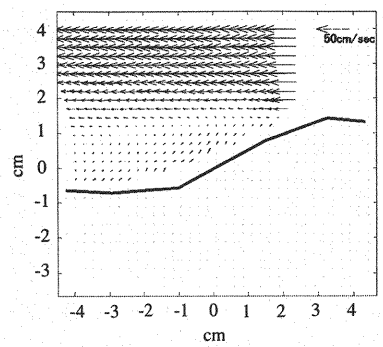

Figure 4: Mean water velocity $\overline{u}_f$ over the rigid dune bed.

both phases are defined by

$$k_f = \frac{1}{2}(\overline{u'_f \cdot u'_f}); R_f = \overline{u'_f v'_f} \tag{6}$$

$$k_s = \frac{1}{2}(\overline{u'_s \cdot u'_s}); R_s = \overline{u'_s v'_s}. \tag{7}$$

The relative velocity between water and sand phases ($\overline{u_r} = \overline{u_s} - \overline{u_f}$), which is a factor in determining particle drag, is also discussed. The above turbulence statistics are examined for both of the RDB and MDB experiments.

RESULTS

The formation of a turbulent shear layer behind both rigid impermeable dunes and sand dunes is discussed, and the effects of the presence of suspended sand particles on the carrier turbulent flow are also discussed by making the comparisons between rigid and mobile dune beds.

Water flow over the rigid dune bed (RDB)

Figure 4 shows the velocity vector of mean water flow ($\overline{u}_f$) passing over the rigid dune crest. The horizontal and vertical coordinates represent a real reference frame of which the origin locates at the point that the dune surface up-crosses an initial bottom level. The same coordinates are used for the rest of the figures. The boundary shear layer is found to separate just behind the crest and to extend horizontally downstream at the level of the dune crest. A weak counter flow appears in the vicinity of the back slope of the dune, and a large-scale rotational flow is observed in the separation region beneath the shear layer.

Strong turbulent energy is produced at the crest, which extends along the separated shear layer with diffusion (see Figure 5). There are high gradients of Reynolds stress from the separation point along the shear layer, indicating that vertical momentum transfers are enhanced across the shear layer.

Sand-laden flow over the mobile dune bed (MDB)

The shear boundary layer is significantly developed on the RDB since the vertical gradient of horizontal

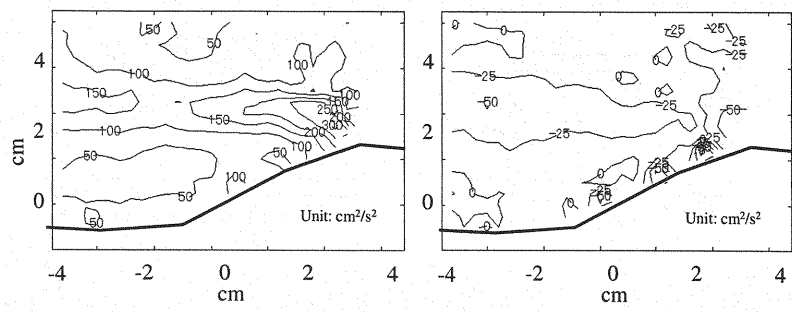

Figure 5: Water turbulent energy (left) and Reynolds stress (right) over the rigid dune bed.

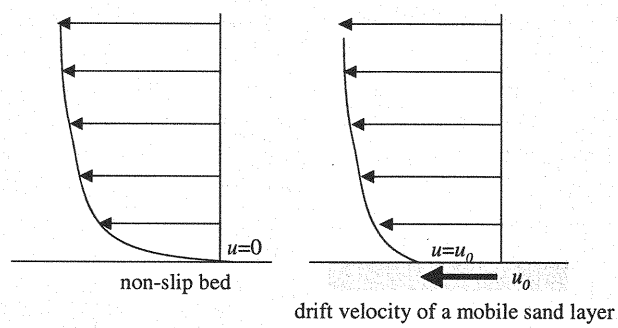

Figure 6: Schematic representation of the velocity profile over the non-slip bed (left) and drifting bed (right). The vertical gradient of horizontal velocity becomes mild on a drifting sand sheet of the MDB.

velocity over the non-slip bottom becomes very high. On the other hand, the development of the shear layer near the MDB is constrained since the upper layer of the sand bed drifts with the water flow to induce a relatively low vertical gradient of horizontal velocity over the bed, as shown in figure 6. Figure 7 shows the mean velocity and turbulent energy for the water phase in the MDB experiment. The separation of the shear boundary layer is found to occur on the back slope of the dune at a level lower than that for the RDB. The separation region becomes relatively small and no counter flow is observed in this region, unlike in the RDB experiment (Figure 4). On the other hand, a downward water flow appears under the shear layer over the dune trough, and this flow is induced in the settling process of the suspended sand particles, which will be explained later. While the turbulent energy near the separation point of the weak shear layer is much lower than that for the RDB (see also Figure 5), the turbulent energy gradually intensifies over a wide region over the dune trough, a feature that is opposite to that in the RDB case, in which turbulent diffusion is enhanced downstream of the shear layer. It is speculated that the suspended sand particles released near the separation point behind the crest induce additional turbulence due to particle drag during the convecting and settling processes, causing modification of the turbulence organization.

The sediments are driven due to the drag receiving from the carrier flow, while the carrier flow around the suspended sediments is locally decelerated via the momentum exchange between the two phases. The dynamic effects of the particle drag, which is proportional to a square of the relative velocity between the water and sand velocities, will be discussed with the measured relative velocity

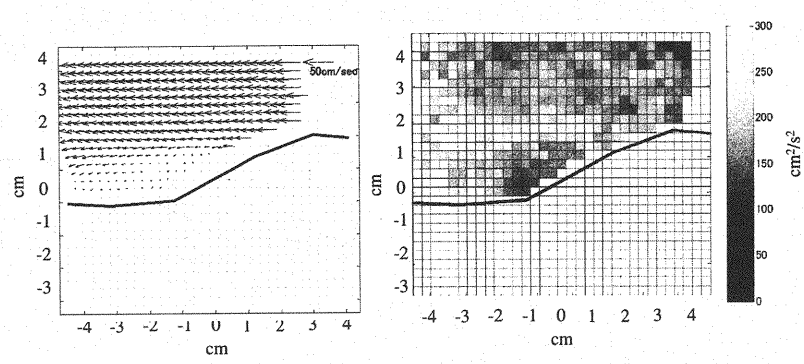

Figure 7: Mean water velocity (left) and turbulent energy (right) over the mobile dune bed.

($\overline{u_r} = \overline{u_s} - \overline{u_f}$). Figure 8 shows the spatial distribution of $\overline{u_r}$ and the number density of suspended sand over the MDB. There is significant horizontal relative velocity in the vicinity of the separation point behind the dune crest and extends along the shear layer, indicating that the sediments are ejected there to accelerate downstream on the layer, and inversely the water flow is locally decelerated along the layer because of the momentum transfer from the carrier flow to the sediments. Findings indicate that the downward drag due to the settling sediments induces the downward flow in the separation region over the dune trough where high concentration of the suspended sediments distributes. In this settling process, the momentum of the suspended sediments is transferred to the water flow in the separation region. The suspended sediments tend to concentrate in a stagnation region of the carrier flow, which might affect flow patterns behind the dune crest.

As mentioned previously, the effects of the presence of suspended sand particles on the momentum transfer (Figure 8) and turbulence structure (figure 7) are the main factors determining underlying features of the sand-laden turbulent flow over the sand dunes. Figure 9 shows the differences in mean water velocity and turbulent energy for the water phase between the RDB and MDB experiments. The horizontal water velocity for the RDB is faster in the region above the crest level than that for the MDB and is inversely slower below that level. This might be caused by the dynamic effects of the suspended sand particles to decelerate the water flow above the shear layer and to accelerate the water flow below the layer, as aforementioned. In this case, the momentum of the water flow, transferred to drive the sediments in the settling region over the dune trough, is estimated to about 20%. In the settling region, the turbulent energy for the MDB is found to significantly intensify to over five-times higher than that for the RDB (see Figure 9). The additional turbulence induced during the settling process may disturb the bed surface and enhance resuspension of the disturbed sand particles (see the resuspension region about x ~-4 cm in figure 7 right), and then the resuspended sand particles may recursively modify the local carrier turbulent flow. The recursive momentum exchanges between the sand and water phases via suspension, diffusion, settling and resuspension processes characterize sand-laden turbulent flows over mobile sand dunes.

It should be noted that the above discussions are concerned with flow modifications by suspended sediments under the same inflow discharge, but the same mean velocity (the mean velocity in the RDB is faster than that in the MDB since the water depths in the RDM and MDB are different under the same discharge).

Further experiments need to be done to determine a relation of flow structures and concentration

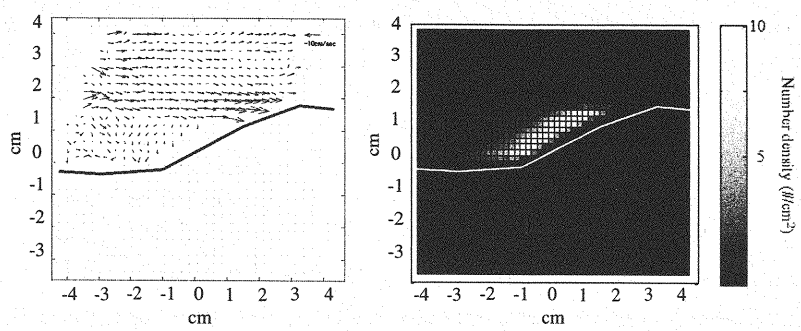

Figure 8: Relative velocity $\overline{u_r} = \overline{u_s} - \overline{u_f}$ of the mean water and sand velocities (left) and the mean number density of suspended sand (right) for the MDB.

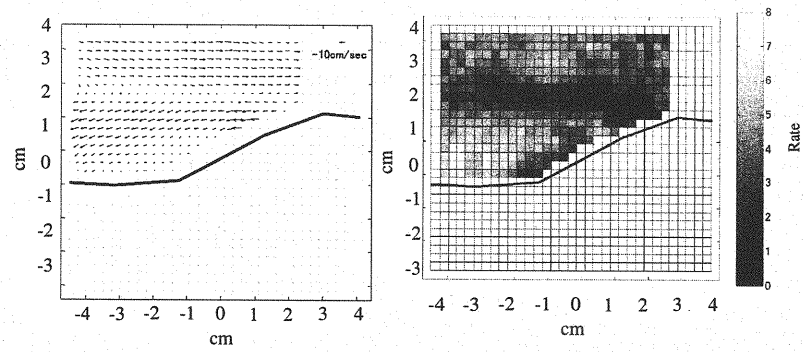

Figure 9: Difference in mean water velocity between the RDB and MDB (left, $\overline{u_f}|_{MDB} - \overline{u_f}|_{RDB}$): rate of turbulent energy for the MDB to that for the RDB (right, $\frac{k_f|_{MDB}}{k_f|_{RDB}}$).

of suspended sand.

CONCLUSIONS

In this study, momentum exchanges between water and suspended sand particles via water-sand interactions in open channel flows over sand dunes are discussed by making comparisons of the measured velocities for both phases over rigid and mobile dune beds. The velocities for water and sand phases at the same locations were simultaneously measured by a double camera PIV system and by using an optical resolution technique.

Since the development of a shear boundary layer formed behind the dunes is constrained over a mobile bed, the turbulent energy on the separated shear layer is much lower than that for the rigid dune bed. While drag acting on the sand particles decelerates the water flow above the shear layer at the inception of sand suspension, it accelerates the water flow downward in a settling phase. Additional turbulent energy is induced during the sand settling process, and this additional turbulent energy is over five-times higher than that for the rigid dune bed. This additional turbulence may recursively disturb the bed surface and enhance resuspension of the disturbed sand particles. The recursive momentum exchanges

between the sand and water flows via suspension, diffusion, settlement and resuspension processes play important roles in the determination of sand-laden flows over mobile sandy dunes.

REFERENCES

1. Gore, R. A. and Crowe, C. T. : Effect of particle size on modulating turbulent intensity, Int. J. Multiphase Flow, Vol. 15, pp. 279–285, 1989.
2. Schmeeckle M. W., Shimizu, Y., Hoshi, K., Baba, H. and Ikezaki S.: Turbulent structures and suspended sediment over two-dimensional dunes, Proceedings of IAHR Symposium on River, Coastal and Estuarine Mophodynamics, pp. 261–270, 1999.
3. Singh, A., Nir, A. and Semiat, R.: Free-surface flow of concentrated suspensions, Int. J. Multiphase Flow, Vol. 32, pp. 775–790, 2006.
4. Nezu, I., Noguchi, K., Yamagami, M., Effects of sediment concentration on turbulent structure in sediment-laden open channel flow over sand dunes, Journal of Applied Mechanics, JSCE, 2006 (in Japanese).
5. Adrian R.J.: Particle-imaging techniques for experimental fluid mechanics, Annu. Rev. Fluid Mech., Vol. 23, pp. 261–304, 1991.

APPENDIX – NOTATION

The following symbols are used in this paper:

C	=	normalized cross-correlation;
f, g	=	image intensity;
C_{max}	=	maximum cross-correction;
Δx, Δy	=	window spacing;
Δt	=	frame interval;
$\boldsymbol{u}$	=	velocity;
$\boldsymbol{u}^*$	=	interpolated velocity;
$\boldsymbol{u}_f$	=	instantaneous fluid velocity;
$\boldsymbol{u}_s$	=	instantaneous sand velocity;
$\overline{\boldsymbol{u}_f}$	=	time mean fluid velocity;
$\overline{\boldsymbol{u}_f}$	=	time mean sand velocity;
$\boldsymbol{u}'_f$	=	fluctuation part of fluid velocity;
$\boldsymbol{u}'_s$	=	fluctuation part of sand velocity;
k_f	=	turbulent energy of fluid;
k_s	=	turbulent energy of sand;
R_f	=	Reynolds stress of fluid;
R_s	=	Reynolds of sand;
$\overline{\boldsymbol{u}_r}$	=	relative mean velocity;

(Received Jun 11, 2008 ; revised Dec 19, 2008)